

Highly Sensitive and Selective Determination of Dopamine Based on Ionic Liquid-Titanium Dioxide/Graphene Oxide Nanocomposite Modified Electrode

Chao-Zhi Lv^{1,†}, Dan Chen^{1,2,†}, Zhong Cao^{1,*}, Feng Liu¹, Xiao-Mei Cao³, Jing-Lin He¹, Wen-Yu Zhao¹

¹ Hunan Provincial Key Laboratory of Materials Protection for Electric Power and Transportation, School of Chemistry and Biological Engineering, Changsha University of Science and Technology, Changsha 410114, PR China

² Hunan Airbluer Environmental Protection Technology CO., LTD, Changsha 410019, PR China

³ College of Chemistry and Chemical Engineering, Hunan Normal University, Changsha 410081, PR China

*E-mail: zhongcao2004@163.com

† These authors contributed equally to this work.

Received: 31 August 2016 / Accepted: 25 September 2016 / Published: 10 November 2016

A composite modified voltammetric sensor for dopamine (DA) was successfully developed, which was based on in-situ electrodeposition of ionic liquids (IL, [BMIM]BF₄)-titanium dioxide (TiO₂) nanoparticles on graphene oxide (GO) modified glassy carbon electrodes (GCE). The surface morphologies of different modified electrodes like GO/GCE, TiO₂/GO/GCE, and IL-TiO₂/GO/GCE were characterized by scanning electron microscopy. The electrocatalytic activities of the corresponding electrodes to dopamine (DA) were investigated using cyclic voltammetry (CV) and differential pulse voltammetry (DPV), indicating that IL-TiO₂/GO exhibited much higher electrocatalytic oxidation activity for DA than GO/GCE and TiO₂/GO/GCE. The response of the IL-TiO₂/GO modified electrode to DA was linear within a range of $8.0 \times 10^{-9} \sim 6.0 \times 10^{-5} \text{ mol} \cdot \text{L}^{-1}$, and the limit of detection was found to be $9.62 \times 10^{-10} \text{ mol} \cdot \text{L}^{-1}$ (S/N=3). Furthermore, the fabricated electrode possessed good selectivity, reproducibility and stability, and was applied to quantitative determination of DA in human serum samples with a recovery rate of 98.6~103.2%. The accuracy of the electrode was also comparable to that of a traditional spectrophotometric method, suggesting that the proposed method was of valuable in practical application on biomedical analysis field.

Keywords: Ionic liquid; Titanium dioxide; Graphene oxide; Electrochemical sensor; Dopamine

1. INTRODUCTION

Dopamine (DA, [4-(2-aminoethyl) benzene-1,2-diol]), a significant catecholamine neurotransmitter [1], is widely distributed in brain tissues and body fluids of mammals, which plays a

pivotal role in central nervous, hormonal, renal and cardiovascular systems. Abnormal DA concentrations in extracellular fluid are related with a variety of diseases, such as Parkinson's disease [2, 3], schizophrenia [4], epilepsy [5], and depression [6, 7], etc. Therefore, it has critical significance on quantitative analysis of DA in body fluids on biological drug control as well as clinical diagnosis fields.

Nowadays, there were some documented methods that have been developed for determination of DA, including spectrophotometry [8], fluorescence analysis [9], capillary electrophoresis [10], mass spectrometry (MS) [11], flow injection [12], high performance liquid chromatography (HPLC) [13, 14], gas chromatography-mass spectrometry (GC-MS) [15], and electrochemical luminescence [16]. Whereas most of these methods had certain constrains such as costly instruments, complicated sample pre-treatment, and multi-step sample preparations. Thus, it is necessary to create a new kind of method like DA sensors which is highly simple, rapid, selective, and sensitive.

Compared with other means, electrochemical methods have drawn considerable attention due to their simple device, easy operation, low cost, and high sensitivity and selectivity [17]. As one knows, dopamine has two hydroxyl groups on benzene ring, which can be oxidized to quinone and then reduced to phenol [18]. Therefore DA can be measured by the electrochemical technique. The composite interface of DA sensors with electrochemical characteristics can be mainly divided into anionic film and cationic film. The anion film can interact with DA through physical adsorption and electrostatic binding in a certain condition, such as 3,4,9,10-perylene tetracarboxylic acid functionalized graphene sheet (PTCA-GS)/multi-wall carbon nanotubes (MWCNTs)/ionic liquid (IL) [19], poly (chromotrope 2B) [20], carbon nanotubes (CNT)-IL-graphene oxide (GO) [21], and thioglycolic acid capped CdTe quantum dots (QDs) [22]. The cationic film can interact with the negatively charged substances through electrostatic attraction. For example, Yan et al [23] developed a method for simultaneous determination of DA, uric acid (UA) and ascorbic acid (AA) through Pd-Pt bimetallic nanoparticles(NPs)/polycation (PDDA)-GS. Vasantha et al [24] employed poly(3,4-ethylenedioxy)thiophene modified electrode also for simultaneous detection of DA and AA. Nien et al [25] reported a poly(acriflavine)-modified electrode for electrocatalytic analysis of DA and AA. However, DA possesses high over-potential and less electron transfer rate, and the oxidation products can contaminate the surface of modified electrode. Meanwhile, the electrochemical detection of DA is influenced by the very close oxidation potential of other species (e.g., UA and AA) coexisted in the biological fluids. Therefore, a highly selective and sensitive method is desired for the determination of DA in the coexistence of other biological species.

Graphene oxide (GO) is a two-dimensional sheet that carbon-based nanomaterials formed by sp^2 bonded carbon atoms, and has various oxygen-containing groups (e.g. hydroxyl, epoxide, and carbonyl groups) on their basal planes and edges. This structural characteristic leads to the especial properties of GO with high electric conductivity, thermal conductivity and good mechanical strength [26, 27]. And the oxygen-containing groups of GO have strong interaction with small polar molecules or macromolecules to form composites [28, 29]. These composites can effectively recognize some substances such as glucose [30], organophosphorus [31], and carbaryl [32], etc.

Ionic liquid (IL) is composed entirely of organic cations with delocalized charges and organic or inorganic anions, which has high conductivity, low vapor pressure, wide potential window, good

thermal and chemical stability, high viscosity and good biological compatibility [33, 34]. IL can be employed as not only the supporting electrolyte but also the active material for the chemically modified electrodes [35]. The ionic liquid electrodes were mainly modified with the following aspects: IL droplets or film [36], IL as a modifier of film electrodes [37], IL as one of the components of carbon paste electrodes [38], IL-CNT composite film [19, 39], and appended IL [40]. No matter what kind of modified electrodes, IL not only acted as an appropriate charge-transferring bridge to accelerate the electron transfer rate, but also exhibited wonderful electrocatalytic and antiscale ability [41].

Recently, titanium dioxide (TiO_2) in various forms like nanoparticles, nanoneedles and nanotubes has been applied to the development of dye-sensitized cells [42, 43], photo-catalyst [44], electrochemical sensor and biosensor [45, 46], etc. Nano- TiO_2 possessed many specific physicochemical properties such as good biocompatibility, strong adsorptive ability, high surface area, thermal stability and non-toxicity [47]. Therefore, a novel composite with good electrochemical activity can be prepared by using ionic liquid combined with nano-titanium dioxide, graphene oxide, and etc. In this work, the nano-composite composed by IL- TiO_2 anchored at GO was achieved by a simple electrodeposition process, which was simply called as "IL- TiO_2/GO ". Because of mutual influence of IL, TiO_2 , and GO, the direct electron transfer between DA and electrode surface can be efficiently achieved. Most importantly, the IL- $\text{TiO}_2/\text{GO}/\text{GCE}$ exhibited high selectivity and good stability, which may allow for its promising application in the examination and diagnosis of dopamine-related disease.

2. EXPERIMENTAL

2.1 Reagents and Apparatus

Graphene oxide (GO) was obtained from Nanjing Voshikura Chemical Co., Ltd (China). Ionic liquids (1-butyl-3-methyl imidazole four fluorine boric acid salt, [BMIM] BF_4 , IL) and dopamine were purchased from Sigma (USA). Ascorbic acid, uric acid, tetrabutyl titanate, potassium ferricyanide, potassium ferrocyanide, potassium iodide, zinc sulfate, sodium nitrite, potassium nitrate, ferrous sulfate, nicotinic acid, glycine, folic acid, L-arginine, L-cysteine, DL-tyrosine, L-alanine were obtained from Sinopharm Chemicals Reagent Co., Ltd (Shanghai, China). Human serums were obtained from Xiangya Hospital, Central South University (Changsha, China). Phosphate buffer solution (PBS) was prepared by mixing solutions of 0.1 M Na_2HPO_4 and 0.1 M NaH_2PO_4 , and the pH value was adjusted with 1.0 M HCl and 1.0 M NaOH. All aqueous solutions were prepared in ultrapure water (resistivity $\geq 18.3 \text{ M}\Omega\text{-cm}$) in this study.

All the electrochemical experiments were performed with an electrochemical workstation (Model CHI-760B, Chen Hua Instrument Co., Shanghai, China) in a conventional three-electrode cell with a modified glassy carbon electrode (GCE, 3 mm in diameter) as a working electrode, a saturated Ag/AgCl as a reference electrode, and a platinum wire as an auxiliary electrode. For cyclic voltammetry (CV), the potential range is -0.2~0.6 V, and the scan rate is 50 mV/s. For differential

pulse voltammetry (DPV), the potential range is 0~0.6 V. A pHs-3C pH meter (Dazhong Instrument Co., Shanghai, China) was used for measuring pH. The surface morphologies of GO/GCE, TiO₂/GO/GCE, IL-TiO₂/GO/GCE were evaluated by a scanning electron microscopy (SEM, JSM-6700, JEOL, Japan).

2.2 Preparation of IL-TiO₂ sol

The glassware was washed in newly prepared aqua-regia ($V_{\text{HCl}} : V_{\text{HNO}_3} = 3:1$), then washed cleanly with ultrapure water. IL-TiO₂ sol solution was prepared by mixing with 8.0 mL ethanol, 15 μL H₂O, 50 μL [BMIM]BF₄ and 150 μL tetrabutyltitanate, keeping stirring at 30 °C for 45 min until the solution become milky colloidal solution.

2.3 Preparation of IL-TiO₂/GO/GCE

Fig.1 shows a schematic diagram for the modification process of the composite electrode of IL-TiO₂/GO/GCE. Firstly, the bare GCE was polished with emery paper and alumina slurries (0.05 μm), and then ultrasonically rinsed in ultrapure water, ethanol and ultrapure water, respectively. The modified electrode was fabricated by dropping 5 μL of GO onto a pre-polished GCE, drying at room temperature to form GO/GCE, and then electrodepositing in the IL-TiO₂ sol solution at a potential of -0.20 V for 80 s. For comparison, TiO₂ modified GO electrode (TiO₂/GO/GCE) was also prepared through the same procedure.

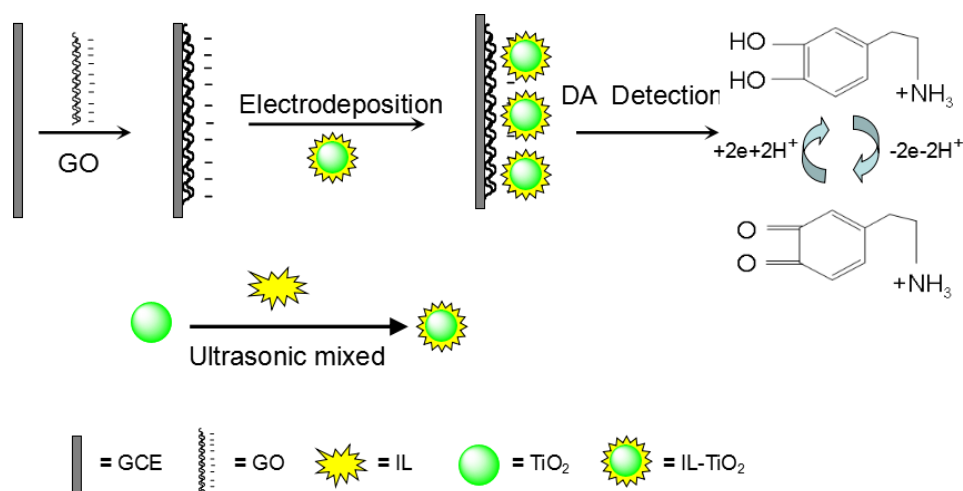


Figure 1. Schematic illustration of IL-TiO₂/GO composite film assembled for detection of dopamine.

2.4 Spectrophotometric method

In order to further validate the accuracy for detection of dopamine in actual samples, a spectrophotometric method was employed. Chromogenic agent solution was prepared as follows: 10.0 mL of phenanthroline (0.02 M), 5.0 mL of Fe(NO₃)₃ (0.01 M), and 2.0 mL of PBS (pH 4.4) were

added into a 25.0 mL volumetric flask, which was diluted to the mark with distilled water. Then, 2 mL of the chromogenic agent solution was added rapidly to 4 mL of standard or sample solutions containing DA. Finally, the absorbance of the solution at $\lambda_{\max}=511$ nm was measured by using a spectrophotometer (Model WFJ-2100, UNICO Shanghai Instrument Co., Ltd, China).

3. RESULTS AND DISCUSSION

3.1 SEM characterization of electrodes

Typical SEM images of the different composite modified electrodes like GO/GCE (A), TiO₂/GO/GCE (B), and IL-TiO₂/GO/GCE (C) are shown in Fig.2. The SEM image presented in Fig. 2A is representative of GO and shows flake-like with wrinkles.

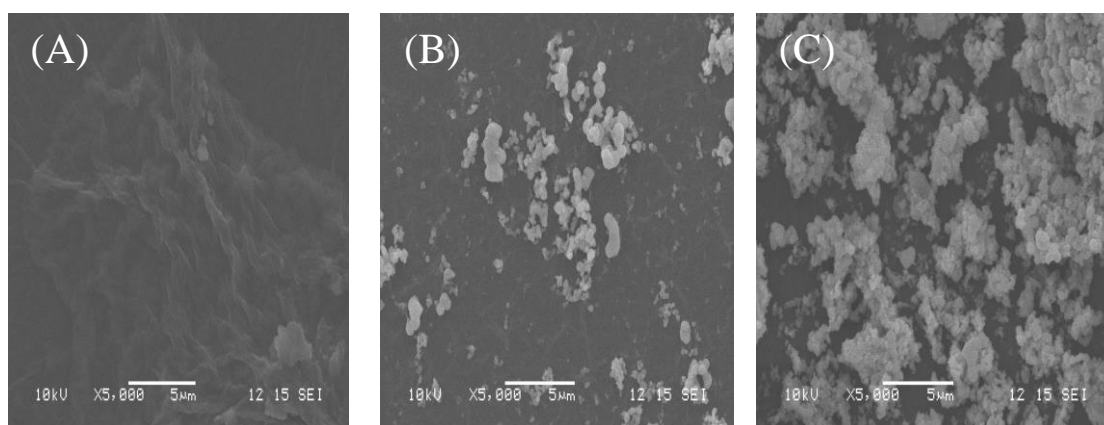


Figure 2. SEM images of the electrode surfaces for GO/GCE (A), TiO₂/GO/GCE (B), and IL-TiO₂/GO/GCE (C).

These structural characteristics of GO can improve the electrical conductivity and the sensitivity of the sensor [48, 49]. Fig. 2B reveals that the distribution of TiO₂ nanoparticles (NPs) on the surface of GO is not uniform, and the amount of TiO₂ NPs is not much. But with addition of IL, the amount of TiO₂ NPs significantly increased and uniformly dispersed on the GO surface as shown in Fig.2C, demonstrating that IL has effectively improved the distribution density and uniformity of TiO₂ nanoparticles. It is mainly due to that it has $\pi \sim \pi$ covalent bonds and strong electrostatic attraction between positively charged IL and negatively charged GO. Once deposited on the GCE surface, IL, TiO₂ and GO tended to form a uniform film on the GCE surface. The uniform surface, along with the high conductivity of IL, TiO₂ and GO, can provide a favorable interface for electrochemical detection of dopamine.

3.2 Electrochemical characteristics of the modified electrode

Cyclic voltammetry (CV) has been employed to examine the assembling process of electrode. Fig. 3 gives the typical CV plots of different modified electrodes like GCE, GO/GCE, TiO₂/GO/GCE,

and IL-TiO₂/GO/GCE in 1.0 mmol/L [Fe(CN)₆]^{3-/4-} containing 0.1 mol/L KCl at the scan rate of 50 mV/s. A pair of distinct redox peaks of [Fe(CN)₆]^{3-/4-} was observed at the bare GCE, indicating a reversible electron transfer process (curve a). But the CV response of [Fe(CN)₆]^{3-/4-} at GO/GCE (curve b) is larger than that of bare GCE, which is attributed to the high electrical conductivity and large specific surface area of GO. After the modification of GO/GCE with TiO₂ (curve c), both the anodic and cathodic peak currents were increased obviously, owing to good catalytic activity and high surface area of TiO₂ nanoparticles. However, when IL-TiO₂ nanoparticles were electrodeposited on the GO/GCE surface (curve d), the redox peak currents of [Fe(CN)₆]^{3-/4-} was further increased at IL-TiO₂/GO/GCE, which is ascribed to good electrical conductivity of IL and well distributed density and uniformity of TiO₂ nanoparticles. Thus, these results indicated that the materials of GO, TiO₂ and IL were successfully modified on the surface of GCE and could accelerate the electron transfer.

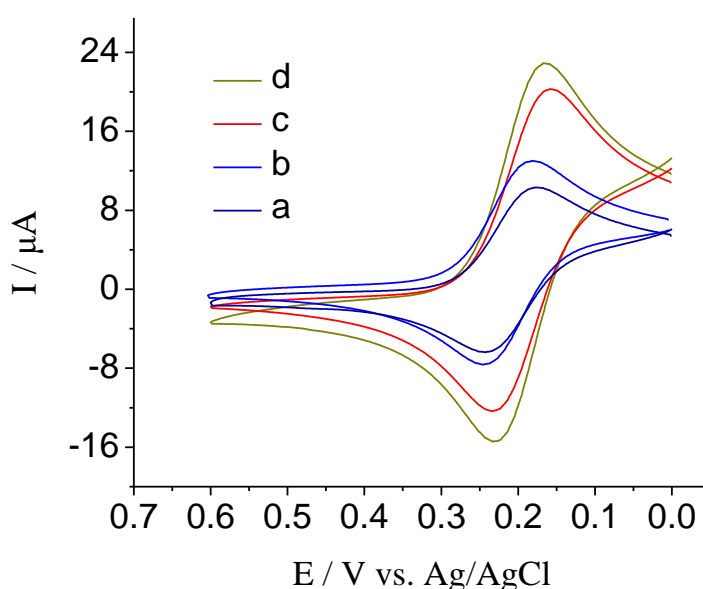


Figure 3. Cyclic voltammograms of bare GCE (a), GO/GCE (b), TiO₂/GO/GCE (c), and IL-TiO₂/GO/GCE (d) in 1.0 mmol/L [Fe(CN)₆]^{4-/3-} solution containing 0.1 mol/L KCl. Scan rate = 50 mV/s.

In order to compare the electrocatalytic properties of the modified electrodes, the active area of each electrode was calculated using Randles-Sevcik equation[50]:

$$I_p = (2.687 \times 10^5) n^{3/2} A C D^{1/2} \nu^{1/2} \quad (1)$$

where I_p refers to the peak current (A) and A is the electrode active area (cm²); D is the diffusion coefficient of the redox probe (6.057×10^{-6} cm²·s⁻¹), C is its concentration (mol/cm³) and ν is the scan rate (V/s). In this work, the active area of GCE, GO/GCE, TiO₂/GO/GCE, and IL-TiO₂/GO/GCE is calculated to be 0.0608, 0.8031, 0.1048, and 0.1456 cm², respectively. The results show that the proposed modified electrode has a larger surface area with good electrocatalytic property, which can improve the adsorption of DA target.

3.3 Electrochemical behaviors of DA

As shown in Fig. 4A, the electrochemical behaviors of DA at different electrodes like bare GCE, GO/GCE, TiO₂/GO/GCE, and IL-TiO₂/GO/GCE were explored by using CV method in 0.1 mol/L PBS (pH=6.0) containing 20.0 μmol/L DA. It can be seen that the peak currents of the electrodes obeyed the order of bare GCE < GO/GCE < TiO₂/GO/GCE < IL-TiO₂/GO/GCE. The bare electrode exhibited weak peak currents under the presence of DA and the difference of peak potential (ΔE_p) between the anodic peak (E_{pa}) and the cathodic peak (E_{pc}) was calculated as 232mV (curve a), indicating the sluggish electrokinetics on the solid bare electrode. The peak current of DA at IL-TiO₂/GO/GCE (curve d) was larger than that of TiO₂/GO/GCE (curve c) and GO/GCE (curve b), and its corresponding ΔE_p was calculated as 64 mV, showing that the electrochemical reaction process of DA was fast and also quasi-reversible. Meanwhile, the IL-TiO₂/GO/GCE possessed much high oxidation peak current and more negative oxidation peak potential of DA, specifying good electrocatalytic ability to the oxidation of DA. Compared with bare GCE, GO/GCE and IL-TiO₂/GCE, the IL-TiO₂/GO/GCE had large conductivity, high specific surface area, and good electrocatalytic activity.

Moreover, the different modified electrodes were also examined in 0.1 mol/L PBS (pH=6.0) containing 20.0 μmol/L DA by using differential pulse voltammetry (DPV) as shown in Fig. 4B. All the modified electrodes exhibited stronger peak currents than that of the bare electrode, and the peak current at IL-TiO₂/GO/GCE (curve d) was larger than that of TiO₂/GO/GCE (curve c) and GO/GCE (curve b) in sequence, which was ascribed to the fast electron transfer rate and superior electrocatalytic oxidation activity of IL-TiO₂/GO/GCE. The test results were also consistent with those by CV.

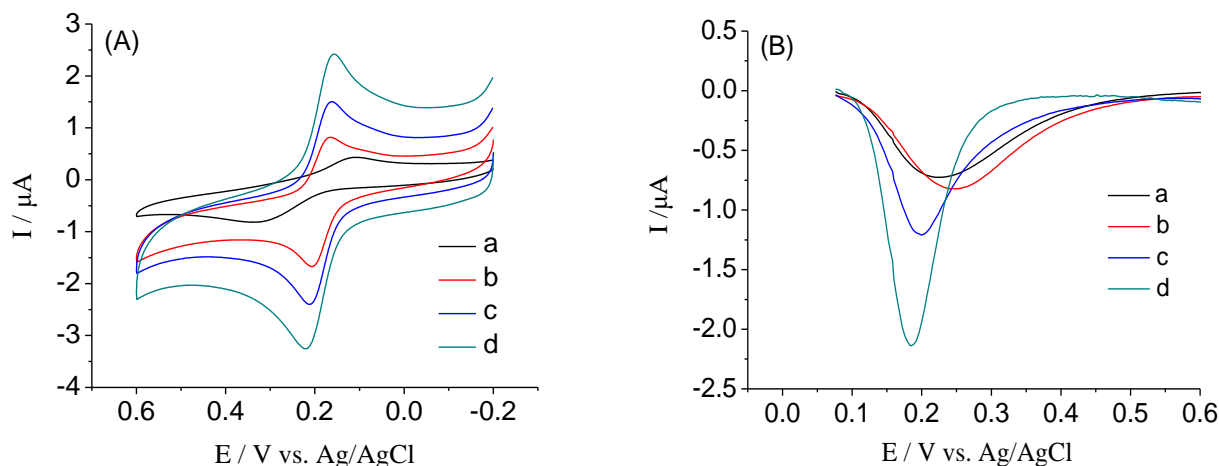


Figure 4 (A) CV responses of bare GCE (a), GO/GCE (b), TiO₂/GO/GCE (c), and IL-TiO₂/GO/GCE (d) in 0.10 mol/L PBS (pH=6.0) containing 20.0 μmol/L DA at scan rate of 50 mV/s. (B) DPV responses of bare GCE (a), GO/GCE (b), TiO₂/GO/GCE (c), IL-TiO₂/GO/GCE (d) in 0.10 mol/L PBS (pH=6.0) containing 20.0 μmol/L DA.

3.4 Optimization of deposition condition

Dosage of GO for the IL-TiO₂/GO/GCE is an important factor which influences the determination of DA. Fig. 5A shows the current responses of 40.0 μmol/L DA at the IL-TiO₂/GO/GCE

which prepared with different dosage of GO. It is found that the maximum current signals can be obtained when the dosage of GO is 5 μL . If the dosage of GO is more or less, the thickness of the film will be fluctuated. It will affect the electron transfer and reduce the catalytic activity to dopamine.

To obtain the optimum electrodeposition time, the redox behavior of 40.0 $\mu\text{mol/L}$ DA at different electrodes was examined by using DPV with the electrodeposition time in 0.1 mol/L PBS (pH=6.0) solution (Fig. 5B). It can be seen that the peak current of DA remarkably increased with the electrodeposition time increased and then decreased with the further increase, and the maximum peak currents was obtained at 80 s. When electrodeposition time exceeded 80 s, the peak current of DA gradually decreased. This may be due to the aggregation of nanoparticles caused by the excessive electrodeposition. Therefore, the electrodeposition time for IL-TiO₂/GO/GCE preparation was set to 80 s.

In the preparation process of IL-TiO₂/GO/GCE, the electrodeposition potential is a factor that cannot be ignored. Fig. 5C shows the peak current of DA at the different IL-TiO₂/GO/GCE prepared with the different electrodeposition potential. When the electrodeposition potential was -0.20V, the peak current of DA was the largest. Hence, -0.20 V was chosen as the optimum electrodeposition potential in the experiment.

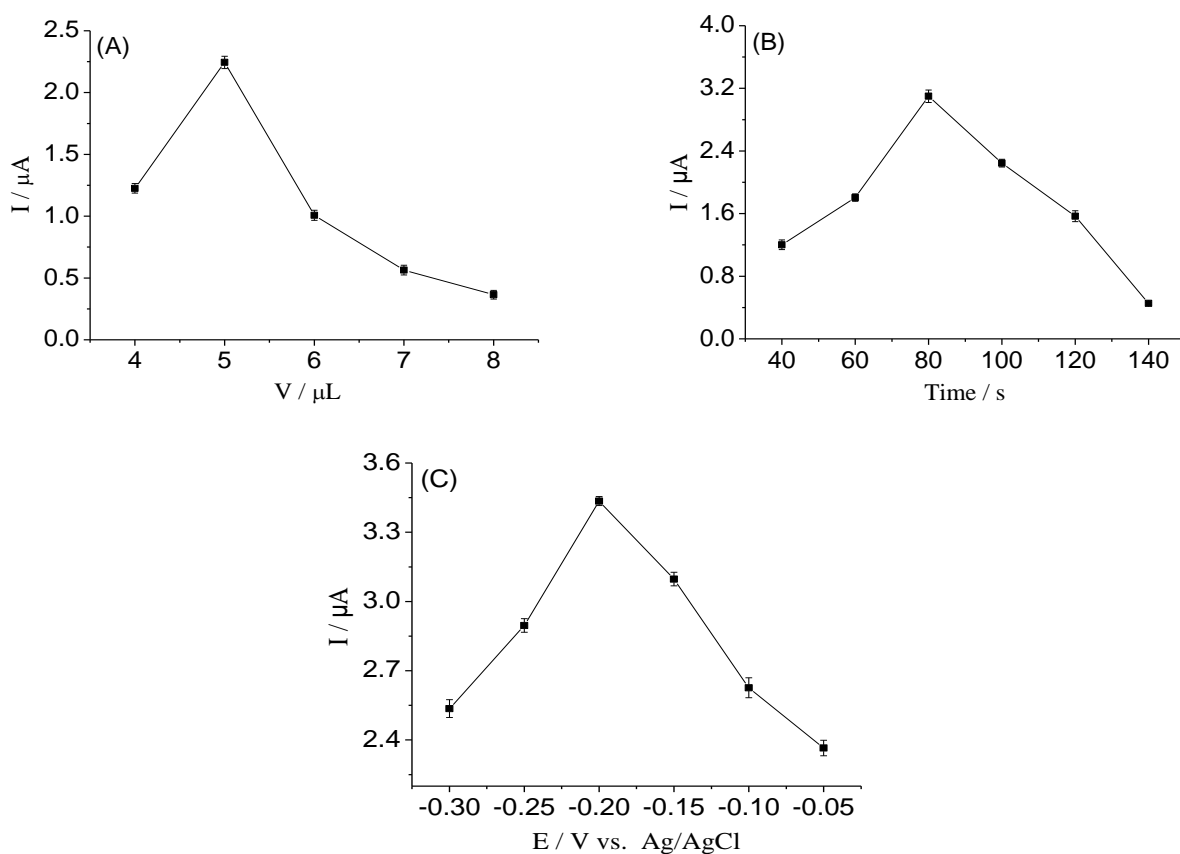


Figure 5. Effects of dosage of graphene oxide (A), electrodeposition time (B) and electrodeposition potential (C) on the peak current with 40.0 $\mu\text{mol/L}$ of DA at IL-TiO₂/GO/GCE.

3.5 Effect of solution pH

Proton is an important factor in the reaction of organic compound which influence the speed. Therefore, the effect of pH on the response of DA was examined over the pH range from 4.0 to 8.0. Plots of peak current against pH are shown in Fig. 6A. The peak current increases with pH ranging from 4.0 to 6.0, and then decreases with pH above 6.0. Thus, the pH 6.0 was chosen for the subsequent analytical experiments, namely in the partial acid condition.

The relationship between the DA peak potential (E_{pa}) and pH was also investigated. One can notice that the peak potential negatively shifts with the pH increased (Fig. 6B), suggesting that the proton is involved in the electrode reactions. The corresponding linear equation can be fitted as follows: E_{pa} (V) = 0.5112 - 0.05052 pH ($r = 0.9987$). According to the theoretical formula: $E_p = E^0 - 0.059 (m/n) \text{pH}$, herein, m is the number of protons transferred in the process of electrode reaction, n is the number of the electrons transferred in the electrode reaction process. Therefore, the curve slope can be calculated, $m/n = 0.8476$, namely $m \approx n$, which shows that the number of electrons and protons involved in the DA oxidation process was equal, that is consistent with the reported literature. For example, the electro-oxidation of DA at poly (chromotrope 2B)-modified GCE [20], graphene/nickel hydroxide/GCE [51], and laser pulse irradiation at GCE [52] were also evaluated to be two electron and two proton processes. The probable reaction mechanism of DA on IL-TiO₂/GO/GCE has been described in Fig. 1.

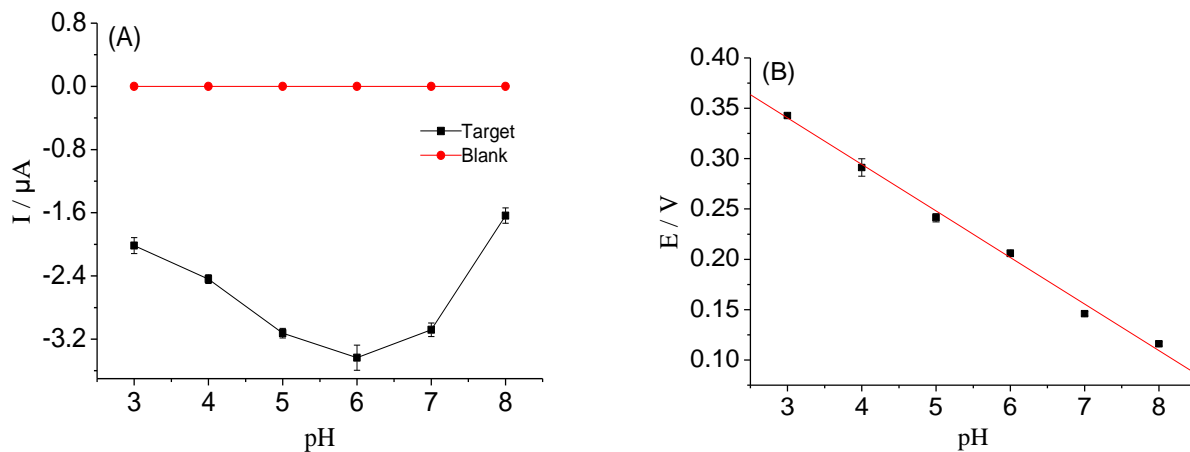


Figure 6. Effects of pH on the oxidation peak current (A) and the oxidation peak potential (B) of DA with 40.0 $\mu\text{mol/L}$ in 0.10 mol/L PBS (pH=6.0).

3.6 Effect of scan rate

The influence of scan rate on the oxidation of DA at the IL-TiO₂/GO/GCE was investigated (Fig. 7). Fig. 7A shows the CVs in 0.1 mol/L PBS (pH 6.0) solution containing 40.0 $\mu\text{mol/L}$ DA with scan rate ranging from 10 to 150 $\text{mV}\cdot\text{s}^{-1}$. The anodic and cathodic peak currents of DA increased simultaneously with the scan rate increased, illustrating that the oxidation process of DA was a completely reversible system on the IL-TiO₂/GO/GCE, while the oxidation peak potentials of DA

gradually positively shifted. In order to determine the number of electrons involved in the slow step of the reaction (n_a) of the IL-TiO₂/GO/GCE electrode, a plot of E_p versus $\ln(v)$ is drawn in Fig. 7B with the linear equation fitted as follows: $E = 0.06614 + 0.02705 \ln(v)$ ($r = 0.9933$). The values of n_a was obtained using Eqs (2) [53]:

$$E_p = E^\ominus - \frac{RT}{2an_aF} \left[0.2691 - \ln \frac{\sqrt{k^0}}{D} + \ln \left(\frac{an_aFv}{RT} \right) \right] \quad (2)$$

where, E_p corresponds to the peak potential, E_0 is the formal potential of the reaction, D is the diffusion coefficient for dopamine, a is the transfer coefficient, v is the scan rate, k^0 is the standard heterogeneous reaction rate constant and n_a corresponds to the number of electrons involved in the slow step of the reaction. R is the universal gas constant, T is the absolute temperature and F is the Faraday constant. By the equation (1) the slope is $RT/2an_aF$. For quasi-reversible system, the electron transfer process is quite slow, so a is 0.5, when $T=298.15K$, and the value of n_a is calculated as 1.88. The result shows that two electrons participate in the oxidation reaction process of DA on the modified electrode.

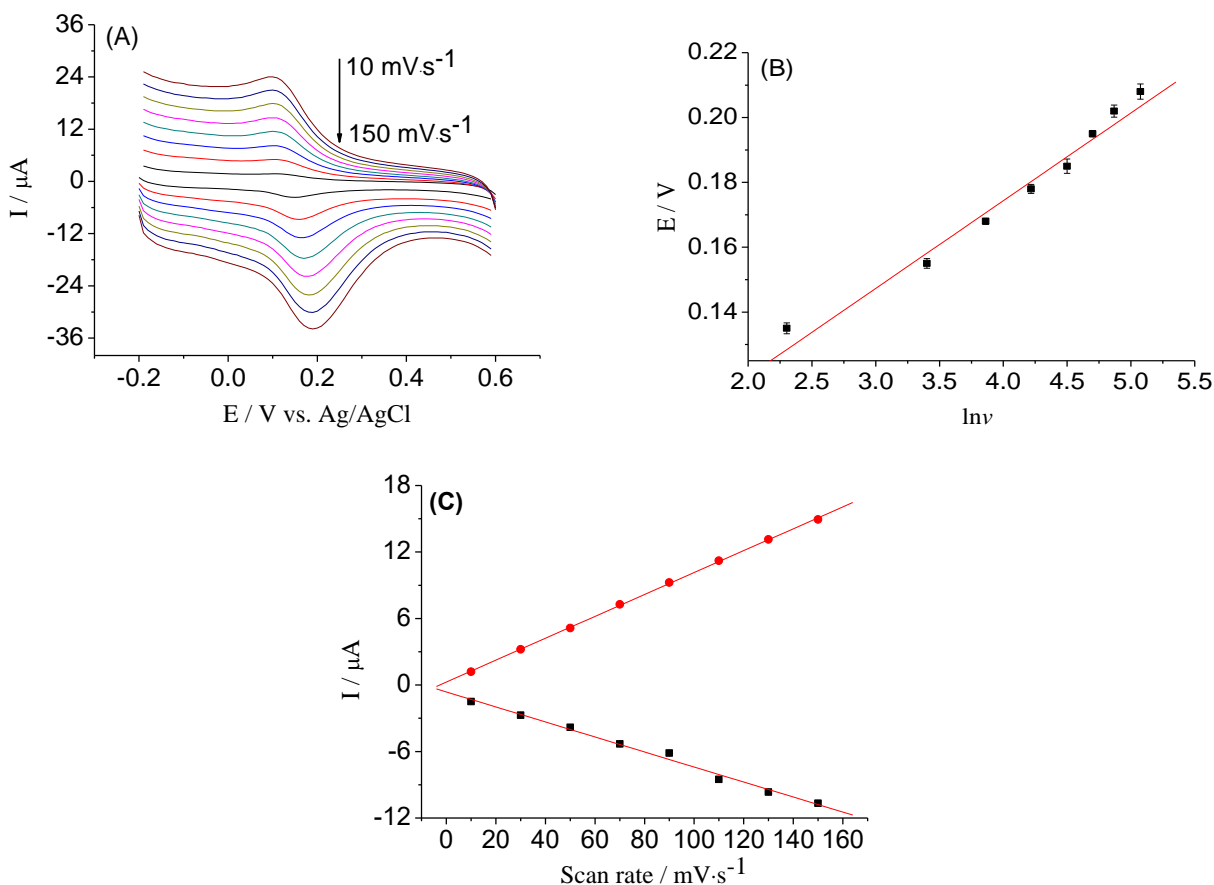


Figure 7. (A) CV plots of IL-TiO₂/GO/GCE in 0.1 mol/L PBS (pH 6.0) containing 40.0 μmol/L DA at different scan rates of 10, 30, 50, 70, 90, 110, 130, and 150 mV·s⁻¹. (B) Plot of oxidation peak potential vs. natural logarithmic scan rate. (C) Plots of cathode and anode peak currents vs. scan rate.

The current response of IL-TiO₂/GO/GCE in 0.1 mol/L PBS (pH=6.0) solution containing 40.0

$\mu\text{mol/L}$ DA was evaluated as a function of scan rate within 10~150 mV/s (Fig. 7C). Both oxidation and reduction currents increased linearly with the scan rate (ν). The linear regression equation can be expressed as I_{pa} (μA) = 0.2675 + 0.09879 ν (mV/s) ($r=0.9998$); I_{pc} (μA) = -0.6223 - 0.06775 ν (mV/s) ($r=0.9989$), thus indicating a adsorption controlled process. As for the peak current is associated with the electrode surface concentration of electroactive material, the value of Γ is obtained by the Eqs (3) [54]:

$$i_p = \frac{n^2 F^2 \Gamma A \nu}{4RT} \quad (3)$$

where, n corresponds to the number of electrons involved in the slow step of the reaction ($n=2$), A is the surface area of the electrode (0.1456cm^2), I_p is the current response value, Γ is the density of the electroactive material (mol/cm^2), ν is the scan rate, F is the Faraday constant, R is the universal gas constant, T is the absolute temperature. So, the value of Γ can be calculated as $1.378 \times 10^{-10} \text{mol}/\text{cm}^2$.

3.7 Linear range and detection limit

Under optimal conditions, the IL-TiO₂/GO/GCE was investigated by DPV responding to various concentrations of DA (Fig. 8A). Based on Fig. 8A, a linear calibration plot was made between the concentrations of DA and the peak currents in Fig. 8B. The results showed that the peak current increased with the DA concentration in the range from $8.0 \times 10^{-9} \text{mol/L}$ to $6.0 \times 10^{-5} \text{mol}\cdot\text{L}^{-1}$ and the regression equation was fitted as I_p (μA) = 0.1112 c ($\mu\text{mol/L}$) + 0.0494 ($r=0.9961$). The detection limit was estimated to be $9.62 \times 10^{-10} \text{mol}\cdot\text{L}^{-1}$ according to a 3:1 signal-to-noise ratio ($S/N=3$). It can be seen that the developed modified electrode exhibits high sensitivity and wide response range, which can be ascribed to the effect of the electrocatalytic ability of IL-TiO₂/GO.

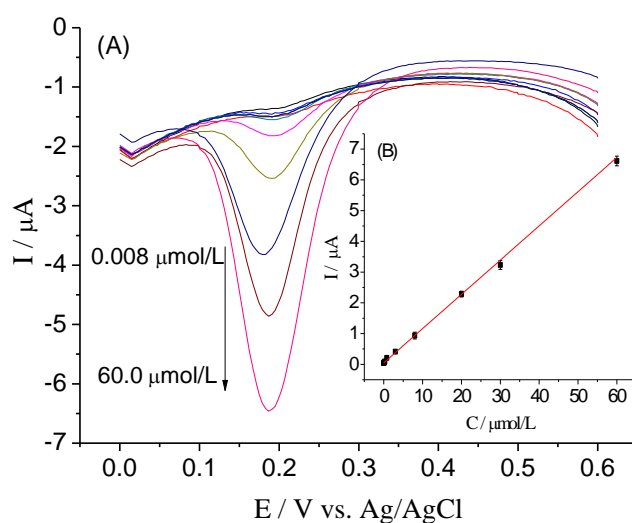


Figure 8. (A) DPV plots of IL-TiO₂/GO/GCE in DA solutions with different concentrations. (B) Relation plot of oxidation peak current vs. concentration of DA.

The main response characteristics of the IL-TiO₂/GO/GCE modified electrode were compared with other different modified electrodes as shown in Table 1. See from Table 1, the detection limit of

$9.62 \times 10^{-10} \text{ mol}\cdot\text{L}^{-1}$ for IL-TiO₂/GO/GCE is much lower than that of others. On the other hand, the detection linear range of $8.0 \times 10^{-9} \text{ mol}\cdot\text{L}^{-1}$ to $6.0 \times 10^{-5} \text{ mol}\cdot\text{L}^{-1}$ has four orders of magnitude, which is relatively very wide. In comparison, the detection limit and the linear range of the IL-TiO₂/GO/GCE modified electrode are much better than that of others reported elsewhere [17, 19, 22, 48, 55-60].

Table 1. Comparison of analytical performance with different modified electrodes.

Electrode	Linear range ($\mu\text{mol/L}$)	Detection limit ($\mu\text{mol/L}$)	Ref.
GR-AuAg/Au	30.0-300.0	20.5	[17]
PTCA-GS/MWCNT/IL/GCE	0.03-3820	0.0012	[19]
TGA/CdTe QDs/Au	0.05-2.0	0.00827	[22]
Trp-GR/GCE	0.5-110.0	0.29	[48]
GR/ β -CD/SPCEs	0.1-58.5	0.011	[55]
rGO-ZnO/GCE	3.0-330.0	1.08	[56]
PPy-IC/GCE	10.0-300.0	0.1	[57]
Fc-S-Au/C-NC/GO/GCE	0.40-645.0	0.08	[58]
OHPMB/rGO/CPE	2.0 - 20.0	0.136	[59]
NiO-CuO/GR/GCE	0.5-20	0.17	[60]
IL-TiO ₂ /GO/GCE	0.008-60.0	0.000962	This Work

Note: β -CD: β -cyclodextrin; CdTe QDs: cadmium telluride quantum dots; CPE: carbon paste electrode; CuO: copper oxide; Fc-S-Au/C-NC: ferrocene derivative stabilized Au NPs/carbon dots; GCE: glassy carbon electrode; GO: graphene oxide; GR: graphene; GS: graphene sheet; IL: ionic liquid; MWCNT: multi-wall carbon nanotubes; NiO: nickel oxide; OHPMB: 2-(2,3-dihydroxyphenyl)4-methyl benzimidazole; PPy-IC: hexagonal-shaped plate-like polypyrrole; PTCA: 3,4,9,10-perylene tetracarboxylic acid; rGO: reduced graphene oxide; SPCEs: screen-printed carbon electrode; TGA: thioglycolic acid; TiO₂: titanium dioxide; Trp: tryptophan; ZnO: zinc oxide.

3.8 Reproducibility

The reproducibility of the IL-TiO₂/GO/GCE was determined towards DA samples in 0.1 mol/L PBS (pH=6.0) solution. Six different modified electrodes prepared under the same condition were applied to detection for DA with 8.0 and 30.0 $\mu\text{mol/L}$, and the corresponding relative standard deviations (RSDs) were 3.72% and 2.02%, respectively. Six parallel detections with the same electrode were also performed to both DA samples, and the RSDs were 2.28% and 1.83%, respectively. Therefore, the proposed IL-TiO₂/GO/GCE had good reproducibility and repeatability.

3.9 Interference

Interference from many foreign species is an important parameter for the DA sensors. The current response of the IL-TiO₂/GO/GCE to 12.0 $\mu\text{mol/L}$ DA was not affected by addition of 100 times of K⁺, I⁻, Zn²⁺, SO₄²⁻, Na⁺, NO₃⁻, NO₂⁻, Fe²⁺, folate, glycine, L-arginine, L-alanine, DL-tyrosine, niacin, 50 times of uric acid (UA), 50 times of ascorbic acid (AA), and 25 times of L-cysteine (Fig. 9). It can be seen that no obvious interference can be observed from these ions and common substance with high

concentration, indicating that the proposed electrode has high selectivity.

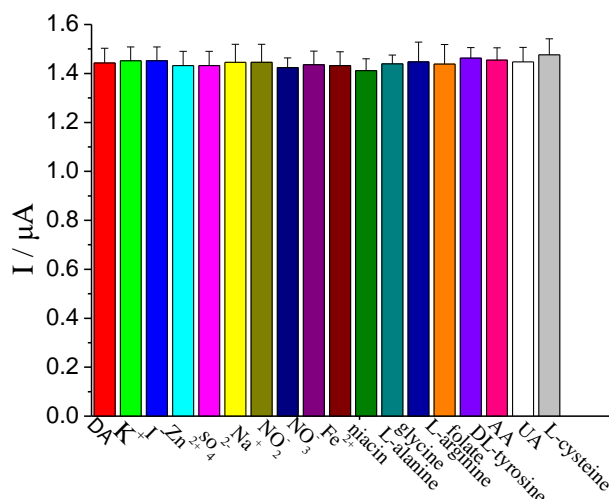


Figure 9. Histogram of electrode for determination of dopamine with co-existing substances: 100 times of K^+ , I^- , Zn^{2+} , SO_4^{2-} , Na^+ , NO_3^- , NO_2^- , Fe^{2+} , folate, glycine, L-arginine, L-alanine, DL-tyrosine, and niacin, 50 times of UA and AA, and 25 times of L-cysteine. The concentration of DA is $12.0 \mu\text{mol/L}$.

3.10 Stability

The stability of the modified electrode varied with the time was evaluated through the DPV. The peak current value retains 99.39% of the initial response signal after 17 days of storage, and 86.9% response signal remained after 21 days of storage, indicating that the proposed electrode was not affected by the DA oxidation products and had excellent long-term stability.

3.11 Determination of dopamine in human serum

In order to verify the practical applicability of the modified electrode, the detection of DA in human serum samples was performed by using IL-TiO₂/GO/GCE. Human serum samples were obtained from Xiangya Hospital, Central South University (Changsha), which were diluted for 25 times with 0.1mol/L PBS (pH=6.0). A series of known concentrations of DA was added to the diluted samples and the corresponding response data were obtained by using DPV. The results were summarized in Table 2. Compared with conventional spectrophotometric method [61], the modified electrode can be efficiently applied to determination of DA in Human serum samples with the corresponding RSD of less than 5%. Moreover, the recovery for the examined serum samples was obtained in the range of 98.6~103.3%, showing that the proposed method possessed good feasibility with potential application value in practice.

Table 2. Determination of DA in human serum samples (n=6).

Sample	Added ($\mu\text{mol/L}$)	Detected by spectro- photometry ($\mu\text{mol/L}$)	Found ($\mu\text{mol/L}$)	RSD (%)	Recovery (%)
Serum 1	2.000	2.034	1.980	4.5	99.0
Serum 2	4.000	3.976	4.131	3.4	103.3
Serum 3	6.500	6.524	6.652	1.7	102.3
Serum 4	9.500	9.639	9.705	2.3	102.2
Serum 5	35.00	35.08	34.51	0.46	98.6
Serum 6	45.00	44.81	46.22	0.52	102.7

4. CONCLUSION

In this work, the ionic liquid-titanium dioxide/graphene oxide (IL-TiO₂/GO) composite was well prepared, and its electrocatalytic oxidation behavior and mechanism toward DA has been investigated in detail. The modified electrode based on IL-TiO₂/GO exhibited excellent sensitivity, selectivity, reproducibility, and stability to the determination of DA with a low detection limit of $9.62 \times 10^{-10} \text{ mol} \cdot \text{L}^{-1}$. The determination results for DA in human serum samples were in agreement with those of spectrophotometric method, illustrating that the proposed electrodes have potential application value in the field of biomedical analysis.

ACKNOWLEDGEMENTS

We are grateful for the financial projects of National Natural Science Foundation of China (Nos. 31527803, 21275022, and 21545010), STS Program of the Chinese Academy of Sciences (No. KFJ-SW-ST5-173), and Foundation of Science and Technology Agency of Hunan Province of China (No. 2015GK1046).

References

1. B. J. Venton and R. M. Wightman, *Anal. Chim. Acta*, 75 (2003) 414.
2. K. A. Jennings, N. J. Platt and S. J. Cragg, *Neurobiol. Disease*, 82 (2015) 262.
3. E. D. M. Rooke, H. M. Vesterinen, E. S. Sena, K. J. Egan and M. R. Macleod, *Parkinsonism Relat. Disord.*, 17 (2011) 313.
4. S. Nakajima, F. Caravaggio, D. C. Mamo, B. H. Mulsant, J. K. Chung, E. Plitman, Y. Iwata, P. Gerretsen, H. Uchida, T. Suzuki, W. Mar, A. A. Wilson, S. Houle and A. Graff-Guerrero, *Schizophr. Res.*, 164 (2015) 263.
5. L. Rocha, M. Alonso-Vanegas, J. Villeda-Hernández, M. Mújica, J. M. Cisneros-Franco, M. López-Gómez, T. C. Zavala, S. C. L. Frías, V. J. Segovia and B. Anna, *Neurobiol. Disease*, 45 (2012) 499.
6. R. Moraga-Amaro, H. Gonzalez, R. Pacheco and J. Stehberg, *Behav. Brain Res.*, 274 (2014) 186.
7. G. Camardese, D. D. Giuda, M. Di Nicola, F. Cocciolillo, A. Giordano, L. Janiri and R. Guglielmo, *J. Psychiatric Res.*, 51 (2014) 7.

8. M.R. Moghadam, S. Dadfarnia, A.M. Shabani and P. Shahbazikhah, *Anal. Biochem.*, 410 (2011) 289.
9. H. B. Wang, H. D. Zhang, Y. Chen, K. J. Huang and Y. M. Liu, *Sens. Actuators B: Chem.*, 220 (2015) 146.
10. Y. S. Zhao, S. L. Zhao, J. M. Huang and F. G. Ye, *Talanta*, 85 (2011) 2650.
11. K. Vuorensola, H. Sirén and U. Karjalainen, *J. Chromatogr. B*, 788 (2003) 277.
12. F. S. Jacobus and S. S. Raluca, *Talanta*, 102 (2012) 34.
13. A. Gottås, Å. Ripel, F. Boix, V. Vindenes, J. Mørland and E. L. Øiestad, *J. Pharmacol. Toxicol. Meth.*, 74 (2015) 75.
14. B. Ferry, E. P. Gifu, I. Sandu, L. Denoroy and S. Parrot, *J. Chromatogr. B*, 951 (2014) 52.
15. N. Attilio, G. Emanuela, S. Giovanni and T. Antonio, *Anal. Chim. Acta*, 810 (2014) 17.
16. D. H. Yuan, S. H. Chen, R. Yuan, J. J. Zhang and X. F. Liu, *Sens. Actuators B: Chem.*, 191 (2014) 415.
17. S. Pruneanu, A. R. Biris, F. Pogacea, C. Socaci, M. Coros, M. C. Rosu, F. Watanabe and A. S. Biris, *Electrochim. Acta*, 154 (2015) 197.
18. D. N. Oko, S. Garbarino, J. M. Zhang, Z. H. Xu, M. Chaker, D. L. Ma, D. Guay and A. C. Tavares, *Electrochim. Acta*, 159 (2015) 174.
19. X. L. Niu, Y. Wu, H. Guo, J. Ren and J. Z. Gao, *Biosens. Bioelectron.*, 41 (2013) 225.
20. X. B. Li, M. Mahbubur Rahman, G. R. Xu and J. J. Lee, *Electrochim. Acta*, 173 (2015) 440.
21. M. L. Wang, Y.Q. Gao, J. J. Zhang and J. W. Zhao, *Electrochim. Acta*, 155 (2015) 236.
22. M. Roushani, M. Shamsipur and H. R. Rajab, *J. Electroanal. Chem.*, 712 (2014) 19.
23. J. Yan, S. Liu, Z. Q. Zhang, G. G. He, P. Zhou, H. Y. Liang, L. L. Tian, X. M. Zhou and H. J. Jiang, *Colloids Surf. B Biointerfaces*, 11 (2013) 392.
24. V. S. Vasantha and S. M. Chen, *J. Electroanal. Chem.*, 592 (2006) 77.
25. P. C. Nien, P. Y. Chen and K. C. Ho, *Sens. Actuators B: Chem.*, 140 (2009) 58.
26. K. N. Spanos, S. K. Georgantzinou and N. K. Anifantis, *Compos. Struct.*, 132 (2015) 536.
27. Y. W. Zhu, S. T. Murali, W. W. Cai, X. S. Li, J. W. Suk, R. P. Jeffrey and S. R. Rodney, *Adv. Mater.*, 22 (2010) 3906.
28. A. D. Dmitriy, S. Stankovich, J. Z. Eric, D. P. Richard, G. H. B. Dommett, E. Guennadi, T. N. SonBinh and S. R. Rodney, *Nature*, 448 (2007) 257.
29. H. Al-Saleh Mohammed, *Synth. Met.*, 209 (2015) 41.
30. M. Li, X. J. Bo, Y. F. Zhang, C. Han and L. P. Guo, *Biosens. Bioelectron.*, 56 (2014) 223.
31. T. Liu, H. C. Su, X. J. Qu, P. Ju, L. Cui and S. Y. Ai, *Sens. Actuators B: Chem.*, 160 (2011) 1255.
32. B. Z. Liu, B. Xiao and L. Q. Cui, *J. Food Compos. Anal.*, 40 (2015) 14.
33. A. Bhattacharjee, J. Lopes-da-Silva, M. G. Freire, J. A. P. Coutinho and P. J. Carvalho, *Fluid Phase Equilib.*, 400 (2015) 103.
34. J. A. Lazzús and G. Pulgar-Villaruel, *J. Mol. Liq.*, 211 (2015) 981.
35. M. Opallo and A. Lesniewski, *J. Electroanal. Chem.*, 656 (2011) 2.
36. J. D. Wadhawan, U. Schröder, N. Andreas, S. J. Wilkins, R. G. Compton, F. Marken, C. S. Consorti, R. F. Souza and D. Jairton, *J. Electroanal. Chem.*, 493 (2000) 75.
37. D. Q. Jin, Q. Xu, Y. J. Wang and X. Y. Hu, *Talanta*, 127 (2014) 169.
38. W. Sun, F. Hou, S. X. Gong, L. Han, W. C. Wang, F. Shi, J. G. Xia, X. L. Wang and G. J. Li, *Sens. Actuators B: Chem.*, 219 (2015) 331.
39. T. Fukushima, A. Kosaka, Y. Ishimura, T. Yamamoto, T. Takigawa, N. Ishii and A. Takuzo, *Science*, 300 (2003) 2072.
40. A. Lesniewski, M. Paszewski and M. Opallo, *Electrochem. Commun.*, 12 (2010) 435.
41. D. Wei and A. Ivaska, *Anal. Chim. Acta*, 607 (2008) 126.
42. Y. P. Liu, S. R. Wang, Zh. Q. Shan, X. G. Li and J. H. Tian, *Electrochim. Acta*, 60 (2012) 422.
43. H. Hua, C. G. Hu, Z. H. Zhao, H. Liu, X. Xie and Y. Xi, *Electrochim. Acta*, 105 (2013) 130.

44. J. J. Murcia, M. C. Hidalgo, J. A. Navío, V. Vaiano, P. Ciambelli and D. Sannino, *Catal. Today*, 196 (2012) 101.
45. W. Sun, Y. Q. Guo, X. M. Ju, Y. Y. Zhang, X. Z. Wang and Z. F. Sun, *Biosens. Bioelectron.*, 42 (2013) 207.
46. Y. Li, H. B. Wang, X. S. Liu, L. Guo, X. L. Ji, L. Wang, D. Tian and X. H. Yang, *J. Electroanal. Chem.*, 719 (2014) 35.
47. X. Chen and S. S. Mao, *Chem. Rev.*, 107 (2007) 2891.
48. Q. W. Lian, Z. F. He, Q. He, A. Luo, K. W. Yan, D. X. Zhang, X. Q. Lu and X. B. Zhou, *Anal. Chim. Acta*, 823 (2014) 32.
49. H. L. Zou, B. L. Li, H. Q. Luo and N. B. Li, *Sens. Actuators B: Chem.*, 203 (2014) 11.
50. C.A. Cordeiro, M.G. Vries, T.I.F.H. Cremers and B.H.C. Westerink, *Sens. Actuators B: Chem.*, 223 (2016) 679.
51. N. T. Mary and K. V. Anitha, *Electrochim. Acta*, 133 (2014) 233.
52. R. S. Rahayu, I. Noviandri, B. Buchari, A. Mikrajuddin and H. Teruo, *Int. J. Electrochem. Sci.*, 7 (2012) 8255.
53. J. Wang, *Analy Electrochemistry*, Translated by Y. C. Zhu and L. Zhang, Chemical Industry Press, Beijing (2008), pp. 29-34.
54. A. P. Brown and F. C. Anson, *Anal. Chim. Acta*, 49 (1977) 1589.
55. S. Palanisamy, S. Sakthinathan, S.M. Chen, B. Thirumalraj, T.H. Wu, B.S. Lou and X.H. Liu, *Carbohydr. Polym.*, 135 (2016) 267.
56. X. Zhang, Y.C. Zhang and L.X. Ma, *Sens. Actuators B: Chem.*, 227 (2016) 488.
57. C.Y. Lee, D.Y. Hsu, A. Prasannan, R. Kalaivani and P.D. Hong, *Appl. Surf. Sci.*, 363 (2016) 451.
58. L. Q. Yang, N. Huang, Q. J. Lu, M. L. Liu, H. T. Li, Y. Y. Zhang and S. Z. Yao, *Anal. Chim. Acta*, 903 (2016) 69.
59. A. Benvidi, S. Dalirnasab, S. Jahanbani, M. D. Tezerjani, M. M. Ardakani, B. Mirjalili and R. Zare, *Electroanalysis*, 28 (2016) 1.
60. B. D. Liu, X. Q. Ouyang, Y. P. Ding, L. Q. Luo, D. Xu and Y.Q. Ning, *Talanta*, 146 (2016) 114.
61. M. R. Moghadam, S. Dadfarnia, A. M. Shabani and P. Shahbazikhah. *Anal. Biochem.*, 410 (2011) 289.